

AD-A155 221

A SIMULATION OF WEATHER IN 3D SPACE(U) AIR FORCE  
GEOPHYSICS LAB HANSCOM AFB MA I I GRINGORTEN 16 OCT 84  
AFGL-TR-84-0267

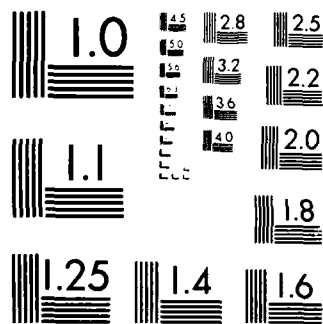
1/1

UNCLASSIFIED

F/G 4/2

NL

									END				
									END				



MICROCOPY RESOLUTION TEST CHART  
NATIONAL BUREAU OF STANDARDS-1963-A

AD-A155 221

# A Simulation of Weather in 3D Space

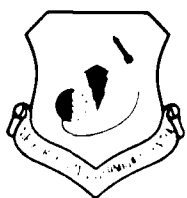
IRVING I. GRINGORTEN



16 October 1984



Approved for public release; distribution unlimited.



DTIC  
ELECTE  
JUN 12 1985  
S D  
G

ATMOSPHERIC SCIENCES DIVISION

PROJECT 6670

**AIR FORCE GEOPHYSICS LABORATORY**


HANSCOM AFB, MA 01731

DTIC FILE COPY

This report has been reviewed by the ESD Public Affairs Office (PA) and is releasable to the National Technical Information Service (NTIS).

"This technical report has been reviewed and is approved for publication"

FOR THE COMMANDER

  
DONALD D. GRANTHAM  
Chief, Tropospheric Structure Branch

  
ROBERT A. McCLATCHEY  
Director, Atmospheric Sciences Division

Qualified requestors may obtain additional copies from the Defense Technical Information Center. All others should apply to the National Technical Information Service.

If your address has changed, or if you wish to be removed from the mailing list, or if the addressee is no longer employed by your organization, please notify AFGL/DAA, Hanscom AFB, MA 01731. This will assist us in maintaining a current mailing list.

Accession For	
NTIS GRA&I	<input checked="checked" type="checkbox"/>
DTIC TAB	<input type="checkbox"/>
Unannounced	<input type="checkbox"/>
Justification	
By _____	
Distribution/	
Availability Codes	
Dist	Avail and/or Special
A/1	

Do not return copies of this report unless contractual obligations or notices on a specific document requires that it be returned.

Unclassified

SECURITY CLASSIFICATION OF THIS PAGE

REPORT DOCUMENTATION PAGE				
1a. REPORT SECURITY CLASSIFICATION			1b. RESTRICTIVE MARKINGS	
2a. SECURITY CLASSIFICATION AUTHORITY Unclassified			3. DISTRIBUTION/AVAILABILITY OF REPORT  Approved for public release; distribution unlimited.	
2b. DECLASSIFICATION/DOWNGRADING SCHEDULE				
4. PERFORMING ORGANIZATION REPORT NUMBER(S) AFGL-TR-84-0267 ERP, No. 892			5. MONITORING ORGANIZATION REPORT NUMBER(S)	
6a. NAME OF PERFORMING ORGANIZATION Air Force Geophysics Laboratory		6b. OFFICE SYMBOL (If applicable) LYT	7a. NAME OF MONITORING ORGANIZATION	
6c. ADDRESS (City, State and ZIP Code) Hanscom AFB Massachusetts 01731			7b. ADDRESS (City, State and ZIP Code)	
8a. NAME OF FUNDING/SPONSORING ORGANIZATION		8b. OFFICE SYMBOL (If applicable)	9. PROCUREMENT INSTRUMENT IDENTIFICATION NUMBER	
8c. ADDRESS (City, State and ZIP Code)			10. SOURCE OF FUNDING NOS	
			PROGRAM ELEMENT NO	PROJECT NO
			62101F	6670
			TASK NO	WORK UNIT NO
			09	10
11. TITLE (Include Security Classification): A Simulation of Weather in 3D Space				
12. PERSONAL AUTHOR(S) Irving I. Gringorten				
13a. TYPE OF REPORT Scientific, Interim.		13b. TIME COVERED FROM _____ TO _____		14. DATE OF REPORT (Yr., Mo., Day) 1984 October 16
15. PAGE COUNT 35				
16. SUPPLEMENTARY NOTATION				
17. COSATI CODES			18. SUBJECT TERMS (Continue on reverse if necessary and identify by block number)	
FIELD	GROUP	SUB GR		
		0402	Simulation Stochastic -Cloud cover	
			Sawtooth wave model CFLOS	
19. ABSTRACT (Continue on reverse if necessary and identify by block number)				
<p>A stochastic simulation process, known as the 3D-Boehm Sawtooth Wave model, has been developed. It has greater versatility than previously applied models. For areal cloud cover, the input consists of the mean sky-cover and a scale parameter, depicted as a characteristic wavelength. The algorithm has been written and programmed to map the simulated clouds horizontally, or in vertical cross-section. Since the model requires climatology in the vertical, a procedure has been developed which takes the cumulative sky-cover as seen by a surface observer and produces estimates of mean cloudiness within any specified layer.</p>				
20. DISTRIBUTION AVAILABILITY OF ABSTRACT UNCLASSIFIED UNLIMITED <input type="checkbox"/> SAME AS RPT <input checked="" type="checkbox"/> DTIC USERS <input type="checkbox"/>			21. ABSTRACT SECURITY CLASSIFICATION Unclassified	
22a. NAME OF RESPONSIBLE INDIVIDUAL Irving I. Gringorten			22b. TELEPHONE NUMBER (Include Area Code) (617) 861-5954	22c. OFFICE SYMBOL LYT

DD FORM 1473, 83 APR

EDITION OF 1 JAN 73 IS OBSOLETE

Unclassified

SECURITY CLASSIFICATION OF THIS PAGE

## Preface

I am indebted to my associates, most particularly to Maj. Albert R. Boehm, USAF, for a careful review and recommended modifications that have been incorporated into this last draft. Maj. Boehm's 3D-Sawtooth Wave Model is basic to the whole procedure.

I must also acknowledge Helen M. Connell's careful preparation of the manuscript.

## Contents

1. INTRODUCTION	1
2. EQUIVALENT NORMAL DEVIATE (END)	3
3. DESIRED MODEL ATTRIBUTES	5
4. THE THREE-DIMENSIONAL BOEHM SAWTOOTH WAVE (3D-BSW) MODEL	9
5. APPLICATION TO SIMULATION	14
5.1 Sample Horizontal Simulation	15
5.2 Sample Vertical Cross-section	16
5.3 Portrayal of Mean Cloudiness - in Layers and at Levels Aloft	18
6. CONCLUSIONS	28
REFERENCES	29

## Illustrations

1. Cumulative Relative Frequency of the January Noontime Visibility at the Bedford, Mass. Airport	3
2. Twenty-four Hour Single-station Precipitation for New England, Based on 27 Januaries (1952-1978)	6
3. Isopleths of 24-hour Precipitation, Drawn to Measured Amounts at 60 New England Stations on 23 Jan 1983	7

## Illustrations

4. Sample Page, From Bertoni and Lund, Showing Temperature Correlations as a Function of Distance Between Stations	8
5. A Plan View and Cross-Section of a Sawtooth Wave Formation	10
6. A 3-Dimensional View of a Point (P) With Cartesian Coordinates (u, v, w), at Distance D From the Origin (0, 0, 0), With Spherical Sides ( $\alpha$ , $\beta$ , $\gamma$ ) and Angular Measure ( $\lambda$ ) From the U-W Plane	11
7. Sample of a Stochastically Generated Field of Clouds in a Horizontal Plane	15
8. Sample of a Stochastically Generated Picture of a Vertical Cross-Section of Clouds	17
9. Another Stochastically Generated Picture of a Vertical Cross-Section, With the Same Conditions as in Figure 8, but Producing Little Cloudiness	18
10. Another Stochastically Generated Vertical Cross-Section, Which Depicts Two Cloud Layers	18
11. An Additional Stochastically Generated Vertical Cross-Section	18
12. The Mean Cloud Cover, From the Ground up to Given Heights for Fort Worth Texas, January, 0300L	21
13. Chart of Mean Cloud Cover in Central Europe, Southern Mountains, January, 0000Z	24
14. Model Estimates of Mean Cloud Cover, for Levels and Layers, for Fort Worth, Texas, January, 0300L	25

## Tables

1. A Typical Set of Values for $h_i$ , $\cos \alpha_i$ , $\cos \beta_i$ , $\cos \gamma_i$ , $i = 1, 12$ , That Were Obtained by Random Process and Used to Obtain Values of $y(u, v, w)$ by Eqs. (17), (16), (19)	16
2. The Areal Coverage A Corresponding to a Ceiling of Clouds Whose Base is at H [Eq. (25a)]	19
3. Sample of Tables Prepared by ETAC on the Frequency of Cloud Amount, $p(f, H)$ Versus Height (H)	20
4. Examples of the Frequency Distribution of Cloud Amount, $p(f)$ , Within a Layer of the Atmosphere	22
5. Presenting the Mean Cloud Cover, $P_O(h)$ in Layers Between 10 Levels Taken in Pairs From 0 ft to 55,000 ft	23
6. Estimates by Eqs. (22) and (24) of the Mean Cloud Cover, $P_O(h)$ , in Layers, Based on the Known Mean Cloud Amounts From the Ground to the Base, $P_O(H)$ , and the Top of Each Cloud Layer, $P_O(H+h)$	26
7. Estimates by Eqs. (22) and (24) of the Mean Cloud Cover, in Layers, $P_O(h)$ , Based on the Given Mean Cloudiness From the Ground to the Base, $P_O(H)$ and the Top of Each Layer, $P_O(H+h)$	27



# A Simulation of Weather in 3D Space

## I. INTRODUCTION

This paper describes a model that stochastically simulates a single-instant set of values of a weather element, both in the horizontal and in the vertical. Using this model, it is possible to generate enough synoptic conditions to collectively provide estimates of the probability distribution of weather events or conditions in 3D space.

In terms of the element cloud cover, it is the goal of this paper to produce a simulated cloud cover, stochastically, that will resemble natural clouds, both in their horizontal extent and in their separation, to include vertical build-up. Eventually this will allow us to provide probability distributions of the amount of cloud cover both in the horizontal and the vertical and of the distances separating clouds.

Stochastic simulation is undertaken in the belief that alternative depictions are not readily available. Theoretically an abundance of observations in the vertical in a small area, in rapid succession, could provide the kind of areal climatology that we seek. Practically speaking, such an abundance would confront us with the prohibitive task of mapping and recording events as a history of the weather, prior to its summarization in statistical format. This is the difficulty that we wish to overcome by modeling. We want to be able to simulate a sequence of changes in the weather covering a given space whenever we choose, and we want, ultimately, to provide usable statistics including correlation coefficients (cc) and probabilities of fractional cover by weather conditions such as cloud cover.

---

(Received for publication 4 October 1984)

With respect to time, most observations might be considered as instantaneous, observed at regular intervals. But there are also time-integrated observations, like 24-hour totals of rainfall. There are observations of the average temperature, and maximum and minimum temperatures in a 24-hour period. All such observations contribute to the climatological character of a location as it relates to the duration of events. Is there a similar climatic record of areal or spatial coverage of climate?

In most previous studies, correlation coefficients (cc) have been the principal object of investigation, with notable exceptions. Schreiner and Riedel<sup>1</sup> collected rainfall data integrated over areas ranging in size from 26 km<sup>2</sup> to 2600 km<sup>2</sup>, and found frequencies of extremes of rainfall as a function of area of the ground covered. Other studies, by Court,<sup>2</sup> Briggs,<sup>3</sup> and Roberts,<sup>4</sup> have linked the rain in a circular area to the central single-station amounts by idealized models. In general, however, efforts to describe areal coverage have been few and models of areal coverage have been rare.

Radar has been a valuable asset in recent years because of the panoramic view that it provides of precipitation within a circular area. Visual satellite imagery, recording as it does the areal cloud cover, eventually should help to provide a 2D cloud climatology. Satellite IR gives the tops but not the internal structure. Satellites and radar, however, are recent tools. Existing climatic records generally contain single-instant observations at single-point weather stations. A recorded rainfall amount is that at a rain gauge. Temperature is that in a thermometer shelter, and so on.

A word should be said about numerical weather prediction (NWP). It would seem that NWP offers an approach to our problem, to generate a sequence of instantaneous horizontal pictures at regular time intervals. This may be done in the future. At this point in time, however, stationarity of NWP models in a statistical sense, is considered unproven and doubtful. The use of NWP to estimate climatic probabilities is expensive and time consuming, yet deficient in supplying climatologies of the items of interest, including cloud cover, ceiling, and visibility. By and large, we must depend on statistical models.

1. Schreiner, L. C., and Riedel, J. F. (1978) Probable Maximum Precipitation Estimates United States East of 105th Meridian, Hydrometeo. Rep. No. 51, NOAA-NWS-RR-51.
2. Court, A. (1961) Area-depth rainfall formulas, J. Geophys. Res., 66:1823-1831.
3. Briggs, J. (1972) Probability of aircraft encounters with heavy rain, Meteorol. Mag., 101:8-13.
4. Roberts, C. F. (1971) A note of the derivation of a scale measure for precipitation events, Mon. Wea. Rev., 99:873-876.

## 2. EQUIVALENT NORMAL DEViate (END)

Before introducing the model, we need to examine the concept of the equivalent normal deviate (END). Single-point frequency distributions, for a variety of weather elements, have been studied in a variety of ways. Generally they do not have a normal distribution. But there always is a value (END) of the normal distribution that has the same cumulative probability as any element value. For example, Figure 1 shows the cumulative relative frequency of visibility, specifically for the January noontime visibility at the Bedford, Mass. airport. Somerville et al<sup>5</sup> have fitted the visibility data to the Weibull distribution, as follows:

$$F(V) = 1 - \exp(-\alpha V^\beta) \quad (1)$$

where, for Bedford, January noontime,

$$\alpha = 0.06906$$

$$\beta = 0.8186 \quad \text{for } V \text{ in miles.}$$

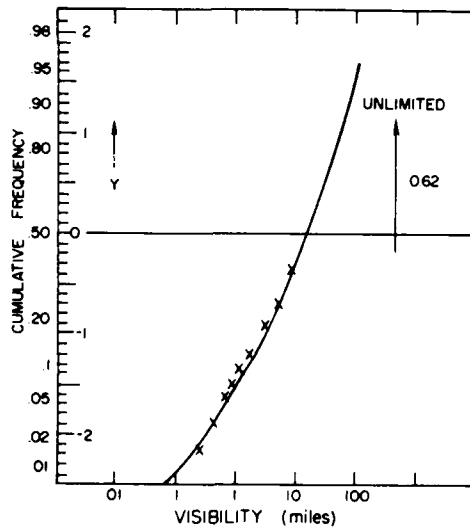


Figure 1. Cumulative Relative Frequency of the January Noontime Visibility at the Bedford, Mass. Airport. The x's mark the frequencies as summarized from 20 yrs of data. They show, for example, a 2 percent frequency for visibility less than 1/4 mile, 7 percent for visibility less than 1 mile, and 38 percent for visibility less than 10 miles, that is, 62 percent frequency of visibility equal to, or greater than, 10 miles

5. Somerville, P.N., Bean, S.J., and Falls, S. (1979) Some Models for Visibility, Scientific Report No. 3, Contract No. F19628-77-C-0080, University of Central Florida, Orlando, Florida, AFGL-TR-79-0144, AD A075490.

The cumulative relative frequency,  $F(V)$ , ranges from 0 to 1. The END-scale of  $F(V)$  is plotted as  $v$  on the graph alongside the probability scale, and ranges from  $-\infty$  to  $+\infty$ . Thus we obtain a transformation of visibility ( $V$ ) into its END ( $y$ ) via  $F(V)$  or vice versa.

Stochastic models derived using the END's instead of the original meteorological variables tend to be more robust and applicable to a greater range of situations. The results are transformed to the appropriate weather variables, when so required.

If we are given the cumulative relative frequency,  $F(x)$  of any variable ( $x$ ), it is defined also as the cumulative relative frequency of the END ( $y$ ). That is,

$$F(v) = F(x).$$

To calculate  $y$  given  $F(y)$ , the National Bureau of Standards<sup>6</sup> provides the approximate formula

$$y = k \left\{ t - \frac{a_0 + a_1 t}{1 + b_1 t + b_2 t^2} \right\} \quad (2)$$

where

$$a_0 = 2.30753$$

$$a_1 = 0.27061$$

$$b_1 = 0.99229$$

$$b_2 = 0.04481$$

$$k = -1, t = \sqrt{\ln \frac{1}{p}} \quad \text{for } p \leq 1/2$$

$$k = 1, t = \sqrt{\ln \frac{1}{(1-p)^2}} \quad \text{for } p > 1/2$$

where

$$p = F(v).$$

6. NBS (1964) Handbook of Mathematical Functions, Applied Mathematical Series, No. 55, Government Printing Office, Washington, D. C.

When the END ( $y$ ) is provided, the corresponding cumulative frequency,  $F(y)$  is approximated by an NBS formula, as follows:

$$F(y) = \frac{1}{2} + m \left\{ 2(1 + c_1 |y| + c_2 y^2 + c_3 |y|^3 + c_4 y^4) \right\}^{-1} \quad (3)$$

where

$$c_1 = 0.196854$$

$$c_2 = 0.115194$$

$$c_3 = 0.000344$$

$$c_4 = 0.019527$$

$$k = 0, \quad m = 1 \quad \text{for } y < 0$$

$$k = 1, \quad m = -1 \quad \text{for } y \geq 0.$$

The cumulative relative frequencies from the observed sample are considered estimates of the cumulative probabilities of the true distribution. If the operative symbol for probability is  $P$ , we assume:

$$P(y) = P(x) = F(x) = F(y). \quad (4)$$

Another example of the transformation of a meteorological element into its END is shown in Figure 2. The END-scale corresponding to the cumulative relative frequency (hence the probability estimate) of 24-hour single-station precipitation is shown for New England, during the month of January.

### 3. DESIRED MODEL ATTRIBUTES

To begin with, the process of generating a model of the areal extent of the weather can resemble a Markov process, but it cannot be one. In a Markov model a future event is dependent upon the present state of the weather and is not additionally governed by events prior to the present. In a horizontal picture, any one point (A) is surrounded by a double infinity of points. There must be, consequently, some underlying restraint on the conditions surrounding A, similar to, but still different from, a Markov process.

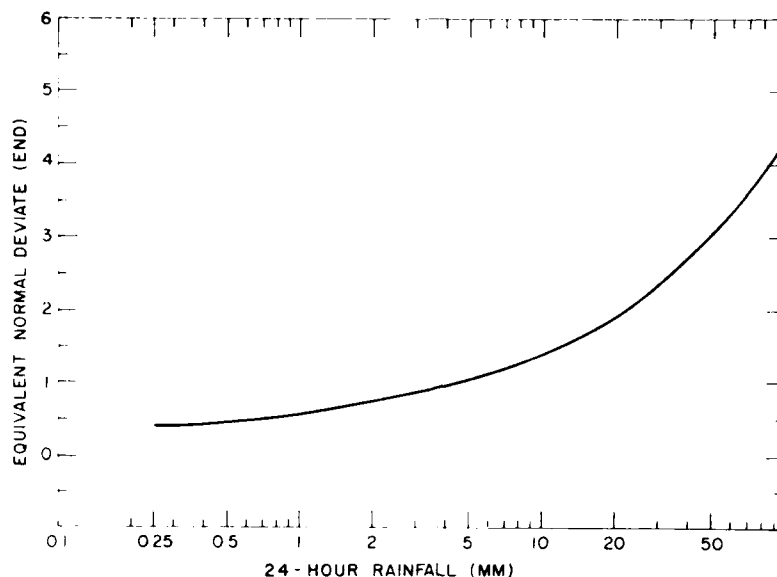


Figure 2. Twenty-four Hour Single-Station Precipitation for New England, Based on 27 Januaries (1952-1978). The ordinate is the uniform scale of  $y$ , the END. The value for zero precipitation is  $y \leq 0.4$ , for 10 mm or less it is  $y \leq 1.4$ , and so on

An effective model of areal coverage will produce a simulated horizontal field, stochastically, that imitates nature but without direct recourse to physical laws or dynamics. An example of the kind of field that the model should simulate is shown in Figure 3. Once a model is selected, the adopted procedure can be repeated many times to produce many simulated synoptic situations, thus comprising a large sample that can be surveyed for spatial correlations or associations of conditions. Therefore, the model must be fast.

The coefficients of correlation of values at two points in the space should generally decrease with increasing distance between the two points in the same manner as nature. Bertoni and Lund<sup>7</sup> have presented results for cc's of pressure,

7. Bertoni, E. A., and Lund, I. A. (1964) Winter Space Correlations of Pressure, Temperature and Density to 16 km; AFCRL-64-1020, AD 611002.

Table 3. Sample of Tables Prepared by ELAC on the Frequency of Cloud Amount, pcf, H Versus Height (H). Figures are for subtotals from the ground up. The example is for Fort Worth, Texas, January, 0300L.

Height (ft)	f = 0 8	1 8	2 8	3 8	4 8	5 8	6 8	7 8	8 8	P <sub>o</sub> Mean
sfc	0.973								0.027	0.027
200	0.973								0.027	0.027
500	0.875	0.011	0.011	0.005		0.011			0.087	0.100
1,000	0.832	0.005		0.005		0.005	0.011		0.141	0.155
1,500	0.766	0.005		0.005	0.005		0.016		0.201	0.218
3,000	0.641	0.005	0.005	0.011	0.016	0.005	0.016		0.299	0.328
5,000	0.598	0.011	0.011		0.016	0.011	0.011		0.342	0.369
8,000	0.549	0.011	0.005		0.022	0.011	0.005		0.397	0.421
10,000	0.544	0.011	0.005		0.016	0.011	0.011		0.402	0.428
12,000	0.500	0.011	0.011		0.022	0.011	0.022	0.005	0.418	0.461
15,000	0.484	0.011	0.011		0.022	0.011	0.022	0.005	0.435	0.478
20,000	0.484	0.011	0.011		0.022	0.011	0.022	0.005	0.435	0.478
30,000	0.397	0.027	0.038	0.016	0.027	0.016	0.027	0.005	0.440	0.507

Observational information on cloudiness has a reasonably high degree of accuracy, as long as it is limited to the determination of ceiling, or the level at which the sky is cumulatively 6/10 covered. There is more information, however, in the daily and hourly observations. In the TDF-14 Airways Observations, the amounts of clouds, in layers, up to four layers aloft, have been recorded. Observers must face the dilemma that lower clouds block the view of higher clouds. It is possible to confidently record the amount of a low cloud. But the amount of cloud in a higher layer could be as low as the extra amount of sky covered by the higher cloud, or could be as high as the total sky covered up to that level.

Table 2. The Areal Coverage A Corresponding to a Ceiling of Clouds Whose Base is at H [Eq. (25a)]

Cloud Height (H)		Areal Coverage (A)
(ft)	(km)	km <sup>2</sup>
	0.1	1.0 (arbitrary)
500	0.15	2.3
1,000	0.30	9.1
3,000	0.91	83.3
5,000	1.52	232
10,000	3.05	925
20,000	6.10	3,641
30,000	9.14	8,050 km <sup>2</sup>

The Environmental and Technical Applications Center (ETAC) of USAF made the latter assumption to provide a distribution of the subtotal cloud cover for 12 levels from the surface to 30,000 ft (Table 3). As long as the item of interest is the sub-total cloud cover, from the ground up to a given level, the assumptions about the hidden clouds are not relevant. As the height is increased the probability of a clear sky (0/8) decreases monotonically, while the probability of (8/8) increases. If  $f$  is the symbol for fractional cover [ $f = 0/8$  (1/8) 8/8], the cumulative probability of the fraction,  $P(\leq f)$ , that is, the amount ( $f$ ), will decrease monotonically with height. (This has been verified in Table 3.)



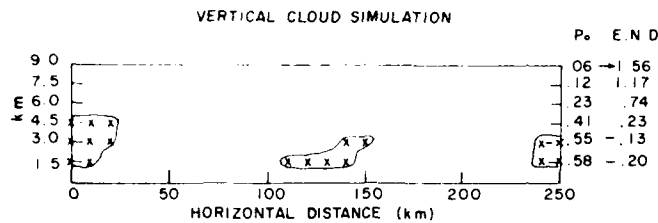


Figure 9. Another Stochastically Generated Picture of a Vertical Cross-Section, With the Same Conditions as in Figure 8, but Producing Little Cloudiness

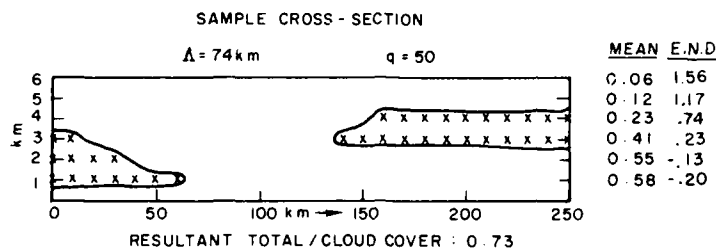


Figure 10. Another Stochastically Generated Vertical Cross-Section, Which Depicts Two Cloud Layers

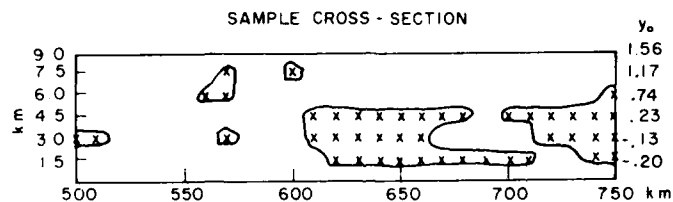


Figure 11. An Additional Stochastically Generated Vertical Cross-Section

### 5.3 Portrayal of Mean Cloudiness—in Layers and at Levels Aloft

As seen above it is necessary that we specify the climatology of cloudiness in selected layers or levels aloft. This section describes a method to estimate the vertical climatology of clouds given standard weather observations.

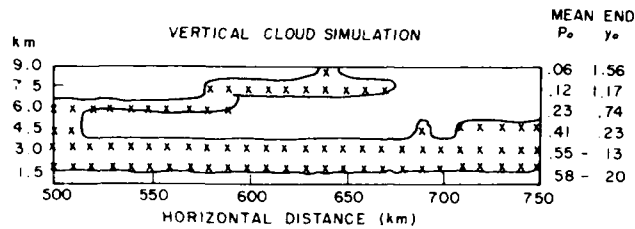


Figure 8. Sample of a Stochastically Generated Picture of a Vertical Cross-Section of Clouds. Chosen:  $\Lambda = 256$  km in the Horizontal. Shrinkage in the vertical:  $1/50$ . Mean cloud cover ( $P_o$ ) varies from 0.58 ( $y_o = -0.20$ ) in the lowest 1.5-km layer to 0.06 ( $y_o = 1.56$ ) in the highest 1.5-km layer. Cloud presence is indicated whenever the simulated  $END(y)$  is greater than  $y_o$ .

The mean cloud cover in the first layer at the location (Central Europe in January) is 0.58, to give the  $END$ ,  $y = -0.20$ . The  $x$ 's, therefore, in Figure 8 were located wherever  $y \geq -0.20$ . In the second layer, from 1.5 to 3 km, the mean cloud cover is 0.55, to give  $y = -0.13$ , and so on. For the top layer, from 7.5 km to 9.0 km, the mean cloud cover is only 0.06 corresponding to  $y \geq 1.56$ , hence there is infrequent cloudiness in this layer.

As opposed to the overcast of Figure 8, another picture, stochastically produced with the same wavelength and mean cloud frequency, resulted in the relatively clear sky of Figure 9. Still another example (Figure 10) produced two layers of clouds, whose total cloud cover was 0.73, compared with the mean total cloud cover for Central Europe of 0.78. Another example (Figure 11) was produced, wherein the random numbers that were used for the horizontal picture of Figure 7 were deliberately used for the vertical cross-section in Figure 11.

The above examples (Figures 7-11) are aimed at producing a picture of a cloudy field, either in the horizontal or in a vertical cross-section. Alternatively, it is possible to imagine that a vehicle's line of travel is plotted, and a determination made as to where, along its path, it penetrates a cloud. So far, it would have to be assumed that the vehicle completes its travel instantaneously, or within a reasonably short interval of time, to avoid considering time changes.

then the cloud boundaries should be found wherever the END  $y = -0.26$ . Hence, the shading, which represents the cloud presence, has been inserted on the figure wherever  $y \geq -0.26$ . Three circles of radius 27.8 km are centered at three supposed observation points, where the observer's sky dome has a radius of 27.8 km (15 nm) or a floor space of 2424 km<sup>2</sup>. At one of the three areas, the observer would see a clear sky, at another a broken sky, and at the third he would record an overcast.

Table 1. A Typical Set of Values for  $h_i$ ,  $\cos \alpha_i$ ,  $\cos \beta_i$ ,  $\cos \gamma_i$ ,  $i = 1, 12$  That Were Obtained by Random Process and Used to Obtain Values of  $y(u, v, w)$  by Eqs. (17), (16), (19)

$i$	$h_i$	$\cos \alpha_i$	$\cos \beta_i$	$\cos \gamma_i$
1	0.3036	0.5159	-0.0994	-0.8509
2	0.4705	-0.2436	0.9699	-0.0050
3	0.1159	-0.1818	0.0045	0.9833
4	0.0944	-0.1183	-0.0069	-0.4044
5	0.9345	0.2931	0.8873	-0.3660
6	0.6600	-0.1013	-0.7891	0.6059
7	0.5655	0.1346	-0.3544	-0.9253
8	0.3212	0.9982	-0.0366	-0.0479
9	0.6899	-0.2305	-0.6861	0.6900
10	0.3618	0.1872	-0.9390	-0.2885
11	0.2223	-0.8925	-0.2022	0.4031
12	0.6509	0.3380	0.4760	-0.8119

## 5.2 Sample Vertical Cross-section

To generate the vertical picture of Figure 8 the wavelength was assumed to be  $\lambda = 256$  km,  $u = 0.010250$  km,  $v = 0$  (for a single cross-section). In the vertical the clouds were generated for six layers of 1.5 km thickness, to make

$$w' = 1.5(1.5)(6) \text{ km}.$$

The END's were found at 26 successive points horizontally for each of the 6 layers aloft. It was assumed that 1.5 km in the vertical was equivalent to 75 km in the horizontal. This makes  $w$ , for our purposes in model application;  $w = q \cdot w'$ . In this example,  $q = 50$ , to give  $w = 75(75)(450)$  km.

### 5.1 Sample Horizontal Simulation

In this example (Figure 7),  $\Lambda = 300$  km,  $I = 10$ ,  $w = 0$ , and  $u, v$  were each given 13 successive values:

$$u = 0(25)300 \text{ km}$$

$$v = 0(25)300 \text{ km}.$$

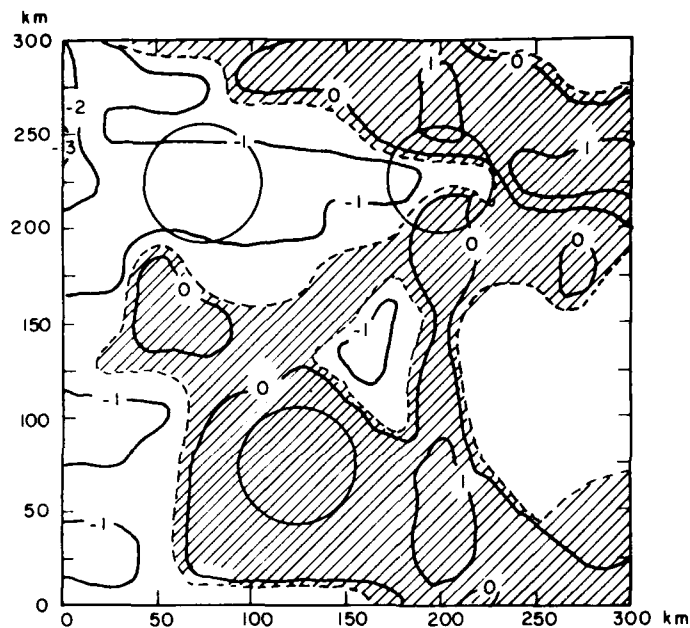


Figure 7. Sample of a Stochastically Generated Field of Clouds in a Horizontal Plane. Chosen:  $\Lambda = 300$  km,  $P_o = 0.6$ , so that clouds are depicted wherever  $y_o \geq -0.26$ . Solid lines indicate constant ENDs; hatching indicates area covered by clouds. Circles indicate three possible areas of radius 27.8 km an observer might see

Using a random number generator, a total of  $12 \times 3 = 36$  random numbers were generated, and then transformed into the numbers (Table 1) that must characterize the resulting field of END- or  $y$ -values. Figure 7 shows the results of drawing isopleths of the END's ( $y$ ) between the ( $13 \times 13 = 169$ ) values generated at the 169 grid points. If, as at Bedford, Mass., in January, the mean cloud cover is 6/10,

If this field is modified by adding a second wave formation to the first, then a pattern will emerge that will be repeated approximately at 1 or 2 wavelengths. If, however, a third wave is added its period will almost always (depending on the random number) be an irrational fraction of the period of the first two waves. As more waves are added the probability of all the waves having rational periods in any given direction is infinitesimal. This implies that, with many wave formations (12 or more) the pattern in any one small area is not likely to be repeated or related in any way to another distant pattern.

## 5. APPLICATION TO SIMULATION

The field characteristic ( $\Lambda$ ) is presumed known, and a simple value (like 10) is assigned to the integer ( $D$ ). The stochastic procedure requires that  $N$  ( $= 12$ , say) wave formations be generated stochastically, which means finding  $N$  sets, each of 3 random numbers, to obtain values [Eq. (15)] for

$$h_i, \cos \gamma_i, \lambda_i, i = 1, N.$$

which, in turn, yield the values [Eqs. (8) and (9)] for

$$h_i, \cos \alpha_i, \cos \beta_i, \cos \gamma_i, i = 1, N.$$

For the point ( $u, v, w$ ) in space [Eq. (17)]

$$D = u \cos \alpha_i + v \cos \beta_i + w \cos \gamma_i \quad (21)$$

to give

$$x_i = FRA (h_i + D/\Lambda + D) \quad i = 1, N \quad (22)$$

to yield the END:

$$y(u, v, w) = \sqrt{\frac{12}{N}} \left[ \sum_{i=1}^N x_i - \frac{N}{2} \right]. \quad (23)$$

To obtain a horizontal picture, stochastically, the distances ( $u$  and  $v$ ) should be chosen at regular grid points, while the vertical height ( $w$ ) should be kept fixed, say at  $w = 0$ . To obtain a vertical picture, one horizontal dimension ( $v$ , say) should be kept fixed, while ( $u, w$ ) are assigned regular gridpoint distances. The result will be a cross-sectional view in the  $U$ - $W$  plane.

Suppose, now, that there are  $N$  formations. Then, at each point  $(u, v, w)$  there will be a set of  $N$  wave phases, whose average

$$\bar{x} = 1/N \cdot \sum_{i=1}^N x_i(u, v, w) \quad (18)$$

will have a mean  $(1/2)$  and variance  $(1/12N)$ . The standardized value at any point,  $y(u, v, w)$ , is given by

$$\begin{aligned} y(u, v, w) &= \sqrt{12N} (\bar{x} - 1/2) \\ &= \sqrt{\frac{12}{N}} \left[ \sum x_i(u, v, w) - \frac{N}{2} \right]. \end{aligned} \quad (19)$$

The sum of  $N$  uniform variables is used to approximate a normal distribution;<sup>9</sup> therefore  $y$  closely approximates an equivalent normal deviate (END).

There will be a value for  $y$  at each and every point in the three-dimensional space. Thus, beginning with  $3N$  random numbers, it is possible to generate a map, or condition or snapshot picture, of END-values in the space to resemble isopleths of temperature, or rainfall, or cloud cover, and so on, at various levels in the atmosphere.

When, for convenience,  $N$  is made equal to 12, the equation becomes

$$y(u, v, w) = \sum_{i=1}^{12} x_i(u, v, w) - 6. \quad (20)$$

For cloud cover, the wavelength ( $\lambda$ ) will be several hundred kilometers in length, while for pressure or temperature fields it will be as much as one thousand kilometers or more in length.

A vertical dimension of 20 km should correspond to a horizontal dimension of, say, 1000 km. That is, if we try, for example, to simulate a horizontal field at sea level, and also the field 1 km above sea level, we might do so by scaling to an effective separation of 50 km. The actual equivalence is yet to be determined.

A question arises about the recurrence of patterns in a given map. In the horizontal, will the picture produced in one small area of the field be repeated in another area? If the procedure stopped with one wave formation, then, as in Figure 5, there would be a regular pattern, with wave phases repeating at distances of 1, 2, --- wavelengths.

9. Enslein, K., Ralston, A., and Wilf, H. (1977) Statistical Methods for Digital Computers, John Wiley and Sons, Inc., New York.

Also since each element is directly proportional to  $\cos \gamma$ , we select  $\cos \gamma$  uniformly:

$$-1 \leq \cos \gamma \leq 1. \quad (13)$$

A wave formation that fills the 3-dimensional space will have three degrees of freedom (two for the angles and one for  $h$ , the phase at the origin). The phase will be uniform between 0 and  $1$ ,

$$0 \leq h \leq 1. \quad (14)$$

Hence, to utilize the three degrees of freedom for the selection of a wave formation, three random numbers ( $R_h, R_\gamma, R_\lambda$ ) are selected to give  $h, \cos \gamma, \lambda$ , each with a rectangular distribution, as follows:

$$\begin{aligned} h &= R_h \\ \cos \gamma &= 2 R_\gamma - 1 \\ \lambda &= 2 \pi R_\lambda. \end{aligned} \quad (15)$$

With a single wave formation there is a determinable value of the wave phase ( $x$ ) at each point ( $u, v, w$ ), as follows:

$$x = FRA (h + D/\lambda + 1) \quad (16)$$

where

$$D = u \cdot \cos \alpha + v \cdot \cos \beta + w \cdot \cos \gamma \quad (17)$$

and where

$$\cos \alpha, \cos \beta \text{ are found by Eqs. (8) and (9).}$$

Now suppose that another wave formation (with the same wavelength  $\lambda$ ) is produced through the choice of three other random numbers. Again there will be a determinable value of the second wave phase at each point ( $u, v, w$ ) but the sum, or average, of the two values will show a more intricate structured pattern than those of one wave formation.

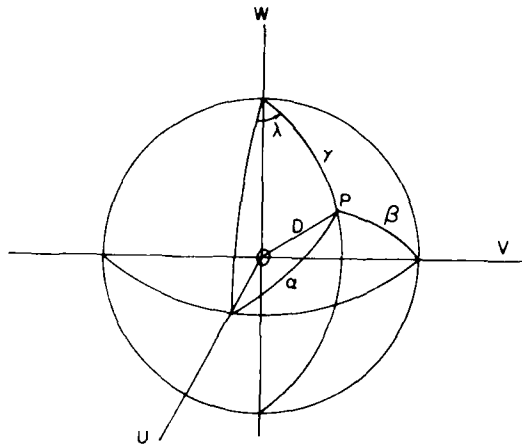


Figure 6. A 3-Dimensional View of a Point (P) With Cartesian Coordinates (u, v, w), at Distance D From the Origin (0, 0, 0), With Spherical Sides ( $\alpha, \beta, \gamma$ ) and Angular Measure  $\lambda$  From the U-W Plane

From the spherical triangles,

$$\cos \alpha = \sin \gamma \cdot \cos \lambda \quad (8)$$

$$\cos \beta = \sin \gamma \cdot \sin \lambda \quad (9)$$

Also,

$$\cos^2 \alpha + \cos^2 \beta + \cos^2 \gamma = 1, \quad (10)$$

which implies that arbitrary choices for sides ( $\alpha, \beta, \gamma$ ) are effectively reduced to two. If  $\lambda$  and  $\gamma$  are selected,  $\alpha$  and  $\beta$  can be calculated by Eqs. (8) and (9).

A sphere of radius D has a surface area of  $4\pi D^2$ . An element of the area ( $\delta A$ ) of this sphere is

$$\begin{aligned} \delta A &= (D \cdot \delta \gamma) (D \cdot \sin \gamma \cdot \delta \lambda) \\ &= D^2 \cdot \delta (-\cos \gamma) \cdot \delta \lambda. \end{aligned} \quad (11)$$

We want each element to be equally probable. Since each element is directly proportional to  $\delta \lambda$ , we select  $\lambda$  uniformly:

$$0 \leq \lambda \leq 2\pi, \quad (12)$$



$$d = u \cos \theta + v \sin \theta , \quad (6)$$

which can be negative or positive.

An integer ( $I = 10$ , say) is added to the sum  $(h + d/\lambda)$  to assure a positive value for  $x$ .

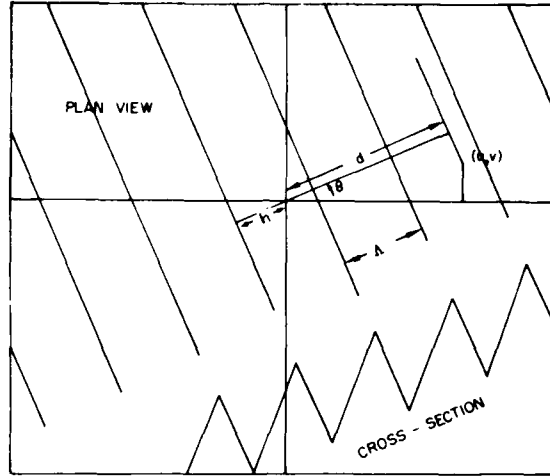


Figure 5. A Plan View and Cross-Section of a Sawtooth Wave Formation

For the 3D BSW model, consider any point (P) with the three coordinates  $(u', v', w')$ . A line from the origin to  $P(u', v', w')$  is oriented with respect to the origin  $(0, 0, 0)$  by angles  $(\alpha, \beta, \gamma)$  between the line and the  $u, v, w$  axes respectively as shown in Figure 6. Consider the plane perpendicular to the line at P. The perpendicular distance of the plane from the origin is  $D$ . From solid geometry, the equation of the plane is

$$u \cos \alpha + v \cos \beta + w \cos \gamma = D . \quad (7)$$

Let  $\lambda$  be the angular measure from the U-W plane to the point P. (If the W-axis were the earth's axis,  $\lambda$  would be the longitude.)

Bertoni and Lund found the cc's for the readily available elements of pressure and temperature, which displayed much persistence. The spatial correlations for phenomena such as precipitation and clouds are expectedly less. The zero correlation distances, compared to those in Figure 4, should be much shorter. An effective model will produce a relation of correlation with distance that will resemble those found from the raw data.

The model needs to be able to give the probability of joint events or events occurring in given fractions of an area or space. For example, cloud cover ranges from clear, through partial cover, to overcast.

#### 4. THE THREE-DIMENSIONAL BOEHM SAWTOOTH WAVE (3D-BSW) MODEL

The objective of the model is to produce, stochastically, on each map or occasion, a correlated field of values of the END similar to the field in Figure 3, and to produce such a depiction at any level, or to produce cross-sectional pictures in the vertical.

Begin with a stationary wave formation that fills the space. Figure 5 shows a plan view, depicting the waves as having a uniform wavelength ( $\lambda$ ). (The formation, at this stage of the explanation, is limited to the two dimensions of the figure.) The leading edge of the middle wave misses the origin of the U, V-axes by the distance ( $H$ ), that is, the phase ( $h$ ) at the origin is  $h = H/\lambda$  and  $0 \leq h \leq 1$ . The orientation of the waves is given by the angle ( $\theta$ ). The values ( $h, \theta$ ) are randomly chosen, but the wavelength ( $\lambda$  km) is a parameter of the model whose length (km or nm) depends on the fluctuation of events in space.

The sawtooth nature of the waves is depicted by their cross-section (bottom of Figure 5). The front edge of each wave has a height of 0, the back edge has a height of 1 and in-between points have a uniform distribution of heights ( $x$ ) where  $x$  is a number from 0 to 1. That is, the height of the wave equals the phase. Thus, at each point ( $u, v$ ) of the space, there is a wave height (or phase) ( $x$ ):

$$x = \text{FRA} (h + d/\lambda + D) \quad (5)$$

where FRA stands for the fractional part of the bracketed sum, and  $d$  is the distance (km) of the wave-phase line from the origin. In the two-dimensional model<sup>8</sup> the distance ( $d$ ) is found to be

8. Burger, C. F., and Gringorten, I. I. (1984) Two-Dimensional Modeling for Lineal and Areal Probabilities of Weather Conditions, AFGL-TR-84-0126, AD A147970.

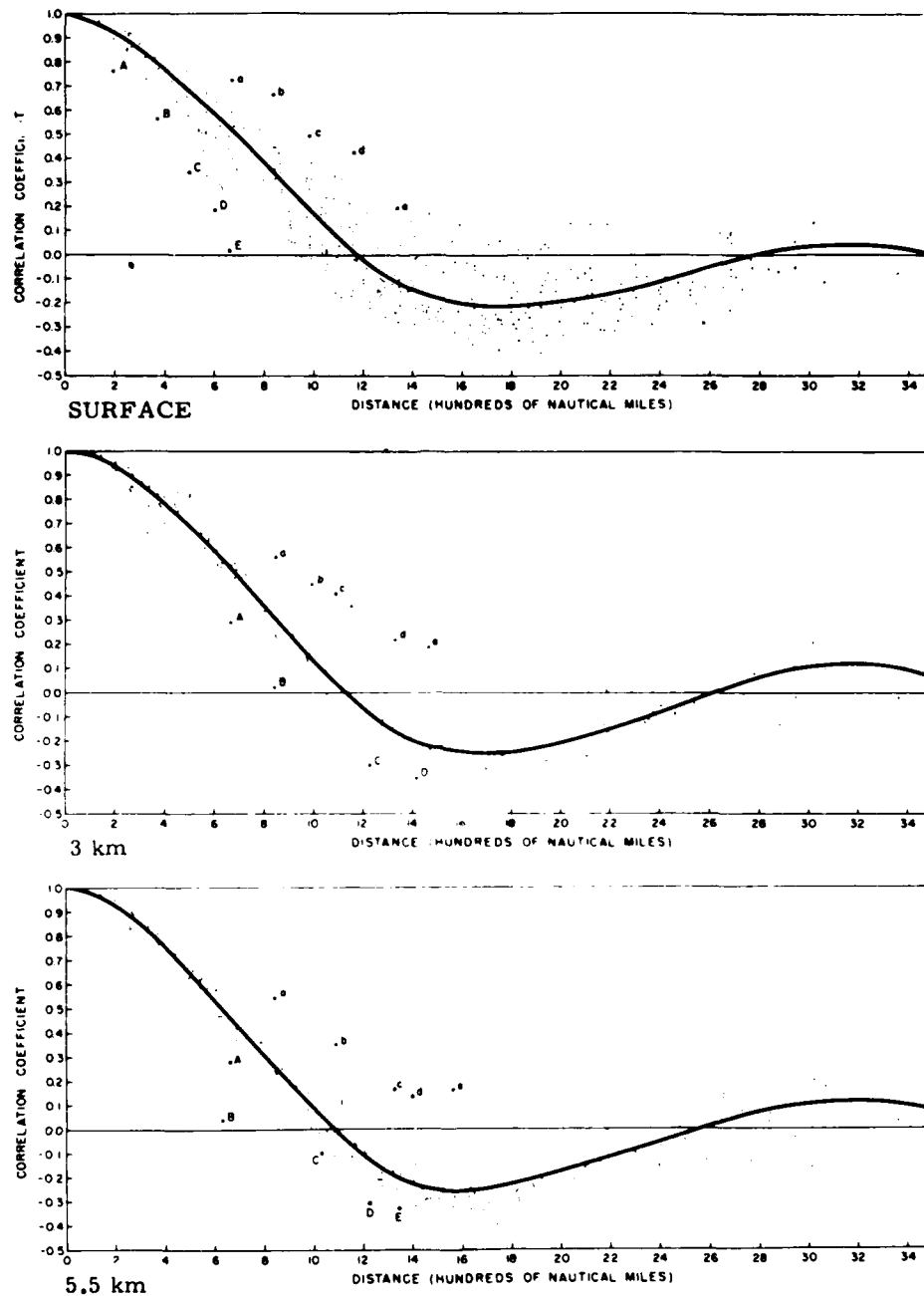


Figure 4. Sample Page, From Bertoni and Lund,<sup>7</sup> Showing Temperature Correlations as a Function of Distance Between Stations

temperature and density at 27 stations taken in pairs at various altitudes in the atmosphere. Figure 4 is a sample page from their report, in which they fitted curves, by eye, to the cc's. The cc decreased with distance, reaching zero at distances of 1000 to 1500 nm. Negative cc's, as low as -0.2, at additional distances of separation of 1000 to 2000 nm, were calculated, after which the cc's were again positive, although slightly.

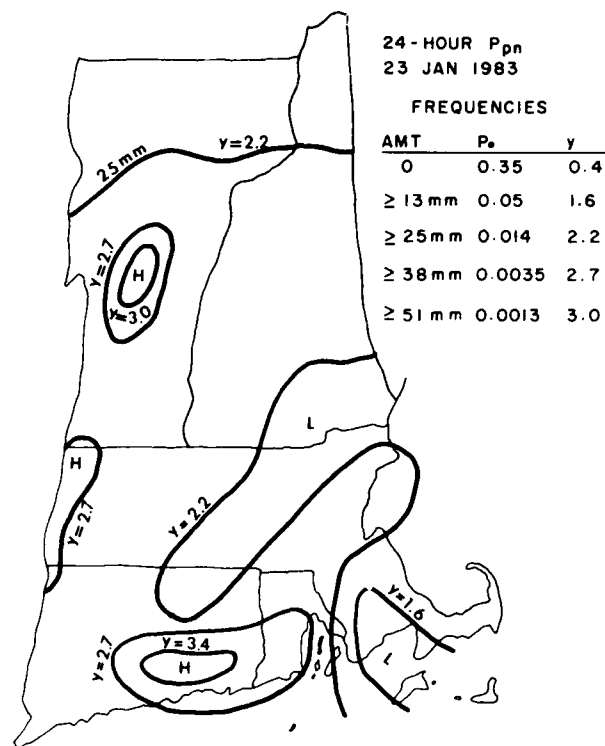


Figure 3. Isopleths of 24-Hour Precipitation, Drawn to Measured Amounts at 60 New England Stations on 23 Jan 1983. Heaviest precipitation is marked H, and lightest L. The amounts on the isopleths, 13, 25, 38, and 51 mm, are exceeded only on 5, 1.4, 0.3 and 0.1 percent of the days respectively based on the climatic frequencies of 27 Januaries (1952-1978). The corresponding END's are  $y \geq 1.6$ , 2.2, 2.7, and 3.0 respectively

Table 3 has the necessary data to find the mean cloud cover from surface to a given height (last column), which increases monotonically with height. This kind of information permits the drawing of one curve in a diagram of mean cloud cover versus height (Figure 12). But there is still a need for more information, for the cloud cover in a layer.

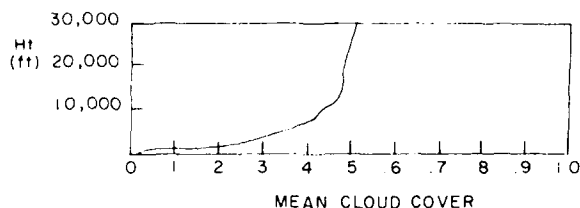


Figure 12. The Mean Cloud Cover, From the Ground Up to Given Heights, Fort Worth, Texas, January, 0300L

DeBary and Moller<sup>10</sup> obtained valuable information on the cloudiness, in layers aloft, through observations made from aircraft flying over Germany. Their study remains unique with respect to the source of data.

For a more universal approach ETAC has used the data of 3D-Nephanalysis as gathered and processed by Global Weather Central. The latter's sources include worldwide surface observations and satellite data. ETAC's data on cloud cover distributions were submitted to us for 45 layers between 10 levels, taken in pairs from the surface to 55,000 ft. Table 4 gives a sample frequency distribution of cloud amount,  $p(f)$ ,  $f = 0(0.1) 1.0$  as estimated within the specified layer.

Table 4 is one of  $(14 \times 45)$  tables, one for each of 7 locations (Korea, north and south; Central Europe, Northern Plains and Southern Mountains; Mid-East, Desert, Eastern Mediterranean and Mountain climates), for each of two mid-season months (January and July) and for each of 45 layers in the atmosphere. Such frequency distribution of cloud amounts yield the mean cloud cover ( $P_o$ ) by the estimate:

$$P_o = \sum_{f=0}^{1.0} p(f) \cdot f \quad f = 0(0.1) 1.0. \quad (24)$$

10. DeBary E., and Moller, E. (1963) The vertical distribution of clouds, J. Appl. Meteorol., 2:806-808.

Table 4. Example of the Frequency Distribution of Cloud Amount,  $p(f)$ , Within a Layer of the Atmosphere. The example is for Central Europe, Northern Plains, January, layer from 1000 to 3500 ft (based on 11 Januaries, 1972-1982)

f	Daytime (12 L)	Nighttime (00 L)
0	0.311	0.380
0.1	0.016	0.015
0.2	0.026	0.013
0.3	0.026	0.022
0.4	0.030	0.018
0.5	0.025	0.021
0.6	0.033	0.024
0.7	0.038	0.027
0.8	0.058	0.037
0.9	0.137	0.099
1.0	0.300	0.345
Mean	0.555	0.525

Table 5 summarizes these estimates of mean cloud cover for all 45 layers, for the same location (Central Europe, northern plains), season (July) and time of day (daytime).

The same kind of information as that found in Table 5 was entered into a chart (Figure 10) and curves drawn (as shown). The curve for layers beginning at 3000 ft was extrapolated downward to that level, thus providing an estimate of the mean cloud cover at that level (0.45). Likewise, other estimates were made for the other levels, and the envelope drawn for the levels. Figure 13 thus provides mean cloud cover at all levels and layers, and is one of 14 such charts that have been drawn to the ETAC data. (The probability estimates of mean cloud cover in Figure 13 were used in the examples of Figures 8-11.)

Table 5. Presenting the Mean Cloud Cover,  $P_0(h)$  in Layers Between 10 Levels Taken in Pairs from 0 ft to 55,000 ft. Example is for Central Europe, Northern Plains, July, daytime

	150 ft	1000 ft	3500 ft	6500 ft	10,000 ft	16,000 ft	26,000 ft	35,000 ft	55,000 ft
0 ft	0.016	0.067	0.467	0.635	0.656	0.713	0.729	0.744	0.747
150 ft		0.066	0.467	0.635	0.656	0.712	0.729	0.743	0.743
1000 ft			0.467	0.635	0.656	0.711	0.727	0.742	0.743
3500 ft				0.607	0.632	0.691	0.707	0.723	0.723
6500 ft					0.430	0.519	0.543	0.561	0.562
10,000 ft						0.348	0.377	0.399	0.400
18,000 ft							0.219	0.248	0.249
26,000 ft								0.150	0.152
35,000 ft									0.033

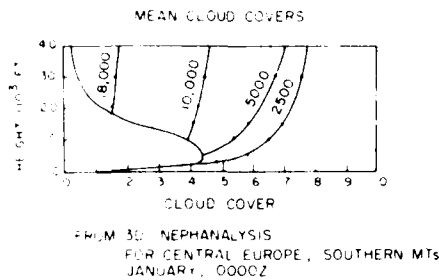


Figure 13. Chart of Mean Cloud Cover in Central Europe, Southern Mountains, January 0000Z. The left-hand envelope gives the mean cloud cover at a level as read on the ordinate. Each branching curve gives the mean cloud cover in the layer between the height as read on the ordinate and the height as marked on the curve

Previously, Gringorten<sup>11</sup> had proposed that the mean cloud cover,  $P_o(h)$ , within a layer of thickness ( $h$ ), be related to the subtotals of mean cloud cover;  $P_o(H)$  and  $P_o(H+h)$ , by the relation:

$$P_o(h) = \frac{P_o(H+h) - P_o(H)}{1 - P_o(H)} \cdot \frac{1}{1 - \exp(-h/G)} \quad (25)$$

If this is accepted, the problem is reduced to finding a suitable expression, or expressions, for the parameter  $G$ . In the previous study, using the deBary and Moller data only,  $G$  could be made a function of  $h$  and  $H$ :

$$G(h, H) = -1.69 + 1.94 \sqrt{H} + 0.475h, \quad G, h, H \text{ in km} \\ = 5.545 + 111.1 \sqrt{H} + 0.475h, \quad G, h, H \text{ in feet.} \quad (26)$$

There was no recognizable relation of  $G$  with season or time of day.

With the later ETAC data the relationship between the parameter  $G$ , the height of the clouds ( $H$ ,  $H+h$ ) and the thickness ( $h$ ) was more readily given as follows:

$$G(h) = \begin{aligned} &890 + 0.30h \text{ ft} && \text{for } H \leq 2500' \\ &6600 + 0.66h \text{ ft} && 2500' < H \leq 9500' \\ &6000 + 1.01h \text{ ft} && H > 9500'. \end{aligned} \quad (27)$$

11. Gringorten, I. I. (1982) Climatic Probabilities of the Vertical Distribution of Cloud Cover, AFGI-TR-82-0078, AD A118753.



Again, as in the previous study, the value of  $G$  could not be systematically related to time of year or time of day, nor could location be clearly associated with the value of  $G$ . The above relations are considered as usable universally. In km:

$$\begin{aligned} G(h) &= 0.271 + 0.30h \text{ km} & \text{for } H \leq 1 \text{ km} \\ &= 2.01 + 0.66h \text{ km} & 1 < H \leq 3 \text{ km} \\ &= 1.83 + 1.01h \text{ km} & H > 3 \text{ km} . \end{aligned} \quad (28)$$

With this formula for  $G$ , Eq. (25) should provide an estimate of the mean cloud cover in any layer, for which no better estimate is available.

To see if Eqs. (27) and (28) are suitable, let us return to the data that ETAC had provided, through use of the TDF 14 (surface) data, as exemplified in Table 3. The mean cloud cover, as plotted in Figure 12, is given only for the whole layer from the ground to levels aloft. The application of Eq. (27) gives the mean cloud cover in layers,  $P_0(h)$ . Table 6 is a record of these estimates, but they are further modified to reduce the estimate in a layer so that it is no greater than the estimate in a thicker layer that contains the thinner layer.

When the estimates of Table 6 are entered into a chart (Figure 14) it appears that there are three modal heights in the distribution of mean sky cover, at 1000 ft, 12,000 ft and 30,000 ft (low stratus, middle clouds and cirrus?).

Since the estimates of Table 6 or Figure 14 are not verifiable with the data on hand, they can be accepted only if they are satisfyingly reasonable. The figures in Table 5 (3D Neph estimates) are available for comparison with the estimates in Table 7. The RMSD of the estimates of mean cloud cover, in 36 layers between 150 ft and 55,000 ft, was found to be 0.066.

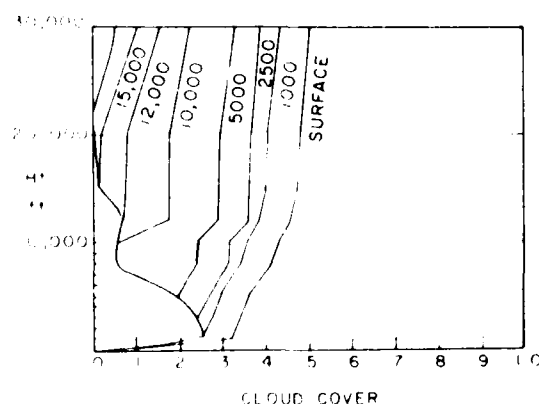


Figure 14. Model Estimates of Mean Cloud Cover, for Levels and Layers, for Fort Worth, Texas, January, 0300L

Table 6. Estimates by Eqs. (25) and (27) of the Mean Cloud Cover,  $P_o(h)$ , in Layers, Based on the Known Mean Cloud Amounts From the Ground to the Base,  $P_o(H)$ , and the Top of Each Cloud Layer,  $P_o(H+h)$ . Example is for the same layer, station, time of year and time of day as in Table 3\*

Lower Level	Upper Level									
	500 ft	1000 ft	3000 ft	5000 ft	8000 ft	10,000 ft	12,000 ft	15,000 ft	20,000 ft	30,000 ft
$P_o =$ sfc	0.100	0.155	0.328	0.369	0.421	0.428	0.461	0.478	0.478	0.507
500 ft		0.155	0.324	0.345	0.393	0.396	0.432	0.445	0.445	0.475
1000 ft			0.277	0.297	0.348	0.352	0.390	0.405	0.405	0.438
3000 ft				0.273	0.321	0.321	0.363	0.363	0.363	0.398
5000 ft					0.236	0.236	0.289	0.289	0.289	0.331
8000 ft						0.054	0.175	0.175	0.175	0.230
10,000 ft							0.175	0.175	0.175	0.230
12,000 ft								0.073	0.073	0.163
15,000 ft									0.000	0.109
20,000 ft										0.058

\* Estimates in any layer are corrected, so that the mean cloud cover in that layer is not greater than the mean in a thicker layer that contains the thinner layer.

Table 7. Estimates by Eqs. (25) and (27) of the Mean Cloud Cover, in Layers,  $P_o(h)$ , Based on the Given Mean Cloudiness From the Ground to the Base,  $P_o(H)$  and the Top of Each Layer,  $P_o(H+h)$ . Example is the same as in Table 5, for comparison with the 3D-Neph estimates\*

Lower Level		Upper Level								
$P_o =$ sfc	150 ft	0.016	0.067	0.467	0.635	0.656	0.713	0.729	0.744	0.747
	1000 ft		0.067	0.467	0.635	0.656	0.713	0.729	0.744	0.747
	3500 ft			0.467	0.635	0.656	0.713	0.729	0.744	0.747
	6500 ft				0.635	0.656	0.713	0.729	0.731	0.731
	10,000 ft					0.177	0.385	0.407	0.429	0.429
18,000 ft						0.382	0.407	0.429	0.429	
26,000 ft							0.129	0.206	0.206	
35,000 ft								0.119	0.119	0.022

\* Estimates in any layer are corrected, so that the mean cloud cover in that layer is not greater than the mean in a thicker layer that contains the thinner layer

## 6. CONCLUSIONS

The immediate goal of simulating a field of weather conditions, specifically cloud cover, has been achieved through use of the "Three-Dimensional Boehm Sawtooth Wave" Model (3D-BSW). It is possible to stochastically simulate a field of clouds, in the horizontal plane or in a vertical cross-section. The simulation is compatible with the basic statistics of cloud cover, including the climatic mean sky cover for a given season and time of day, frequency distribution of cloud cover from clear to overcast, and spatial correlation. This report, however, assumed that the parameters of the 3D-BSW model, the mean cloud cover ( $P_0$ ) and the scale distance or wavelength ( $\Lambda$ ) are known. This report must be followed by another development to present algorithms for the determination of the parameter ( $\Lambda$ ), using published climatological information.

The basic model of this report has been supplemented with supporting models, to extend its use to layers, so that we are able to provide simulation, not only for the total sky cover, but also for a specified layer in the atmosphere. Yet there are many aspects of the problem that must await development.

Certainly the cloud shapes are not simulated in all their picturesque variations. A promising idea along these lines is the simulation of the "fractal" structure of clouds. The characteristics of the separation, or cloud-free intervals, should be simulated, and tested. Instead of a 2-dimensional view, a single line-of-travel, in and out of clouds, could be simulated stochastically, providing a realistic time and duration of exposure of a flying vehicle.

Still to be accomplished is the simulation of a time-lapse sequence of cloud-cover events in three dimensions. Several alternative approaches are possible, including the modeling of the Ornstein-Uhlenbeck process. An investigation into this phenomenon might include the effects of terrain and other geophysical features. When time changes are introduced, the simulation of advection, and cloud types, might also be tried.

## References

1. Schreiner, L. C., and Riedel, J. F. (1978) Probable Maximum Precipitation Estimates United States East of 105th Meridian, Hydrometeo. Rep. No. 51, NOAA-NWS-HR-51.
2. Court, A. (1961) Area-depth rainfall formulas, J. Geophys. Res., 66:1823-1831.
3. Briggs, J. (1972) Probability of aircraft encounters with heavy rain, Meteorol. Mag., 101:8-13.
4. Roberts, C. F. (1971) A note of the derivation of a scale measure for precipitation events, Mon. Wea. Rev., 99:873-876.
5. Somerville, P. N., Bean, S. J., and Falls, S. (1979) Some Models for Visibility, Scientific Report No. 3, Contract No. F19628-77-C-0080, University of Central Florida, Orlando, Florida, AFGL-TR-79-0144, AD A075490.
6. NBS (1964) Handbook of Mathematical Functions, Applied Mathematical Series, No. 55, Government Printing Office, Washington, D. C.
7. Bertoni, E. A., and Lund, I. A., (1964) Winter Space Correlations of Pressure, Temperature and Density to 16 km; AFCRL-64-1020, AD 611002.
8. Burger, C. F., and Gringorten, I. I. (1984) Two-Dimensional Modeling for Lineal and Areal Probabilities of Weather Conditions, AFGL-TR-84-0126, AD A147970.
9. Enslein, K., Ralston, A., and Wilf, H. (1977) Statistical Methods for Digital Computers, John Wiley and Sons, Inc., New York.
10. deBary, E., and Moller, F. (1963) The vertical distribution of clouds, J. Appl. Meteorol., 2:806-808.
11. Gringorten, I. I. (1982) Climatic Probabilities of the Vertical Distribution of Cloud Cover, AFGL-TR-82-0078, AD A118753.

**END**

**FILMED**

7-85

**DTIC**